Physica A 195 (1993) 336–353
North-Holland

SDI: 0378-4371(92)00283-I

PHYSICA A

Viscoelasticity of polymeric melts and concentrated solutions. The effect of flow-induced alignment of chain ends

Martin Kröger[1] and Siegfried Hess

Institut für Theoretische Physik, Technische Universität Berlin,PN 7-1, Hardenbergstraße 36, W-1000 Berlin 12, Germany

Received 24 August 1992

The viscous properties of polymeric liquids and the underlying microscopic distribution function for the segment orientations are investigated by a Fokker–Planck approach. The solution of the Fokker–Planck equation depends on the alignment of chain ends under shear flow, which is usually disregarded. However, it has been inferred from nonequilibrium molecular dynamics (NEMD) computer simulations that it is nonzero. Since the viscous properties depend critically on the magnitude of this end alignment it has been taken into account in the theoretical description. This turns out to be crucial for the plateau region and the high frequency behavior of the complex viscosity. The results are in good agreement with experimental data. Furthermore a significant chain length dependence of the viscous behavior is found.

1. Introduction

Rheological consequences of the concepts of "tube constraint" and "reptation" introduced by Edwards [1] and de Gennes [2] for the dynamics of polymeric melts and concentrated polymer solutions have been investigated by Doi and Edwards [3] and by Curtiss and Bird [4]. It is the purpose of this article to present results for the viscoelasticity as expressed in terms of the frequency dependence of the viscosity or the loss- and storage moduli based on a modified reptation model. Point of departure is the Fokker–Planck equation for the segment orientation based on a bead-rod model. A one-dimensional diffusion (reptation) of chains through their tubes and orientational diffusion of segments are taken into account as damping mechanisms. An equation of change for the alignment tensor is derived, which, in turn, is associated with the friction pressure tensor. Besides a stationary solution of this equation,

[1] Corresponding author.

subject to the Doi–Edwards boundary condition, i.e. random orientations of the end segments of a chain, an alternative solution is presented which takes into account the alignment of chain ends under (oscillatory) shear flow. The finite alignment of the chain ends is substantiated by nonequilibrium molecular dynamics (NEMD) computer simulations. The frequency dependence of the viscosity, obtained by the modified dynamic model, is in better agreement with experimental data than that based on the Doi–Edwards boundary condition.

This article is organized as follows: starting from the freely jointed bead-rod chain model as an idealization of the molecules in a polymeric fluid, we introduce a distribution function for the orientations of segments within one chain. The connection between segment orientation and the friction pressure tensor is taken to be in accordance with the stress optical law which involves the (2nd rank) alignment tensor. An equation of change for the alignment tensor is obtained from a kinetic equation which takes into account a reptation model damping term and orientational diffusion of segments in addition to the contributions which stem from an external flow field. In the case of oscillatory shear flow, the differential equation for the alignment tensor is solved with arbitrary boundary conditions, i.e. we made no restrictions for the alignment of chain ends. The analytical solution yields the frequency dependency of the complex viscosity and we show that it reduces to the expression given by Doi and Edwards if the chain ends are restricted to be non-aligned. After some general remarks on the NEMD method, we discuss the dependency of the anisotropic components of the alignment tensor on both the flow field and the position within the chain which can be compared with the theoretical result. Since the effect of flow-induced alignment of chain ends is confirmed, we discuss its consequence for the complex shear moduli, the width of a plateau region and the asymptotic frequency behavior. We also compare our result with experimental data on polymeric melts and concentrated solutions and give the expressions how to predict the molecular weight dependency of the viscoelastic behavior and how to extract the few theoretical parameters from an oscillatory shear flow measurement.

2. Theory

2.1. Connection between the segment orientation and the friction pressure tensor

The macromolecules of a polymeric liquid are idealized as freely jointed bead-rod chains where the direction of the link between two neighboring beads is characterized by the unit vector $\hat{\boldsymbol{u}}$. The label s (with $0 \leqslant s \leqslant L$ where L is the

length of the chain) marks the position of a specific segment. The orientation of the segment at the "position" s is determined by the orientational distribution function $f = f(t, s, \hat{\boldsymbol{u}})$, which, in general, also depends on the time t. With the normalization $\int f \, \mathrm{d}^2\hat{\boldsymbol{u}} = 1$, the average $\langle \psi \rangle$ of a function $\psi = \psi(\hat{\boldsymbol{u}})$ is, as usual, given by

$$\langle \psi \rangle = \int \psi f \, \mathrm{d}^2\hat{\boldsymbol{u}} \, . \tag{1}$$

Notice that $\langle \psi \rangle$, in general, depends on t and s. Here, the (2nd rank) alignment tensor

$$\boldsymbol{a} = \langle \overline{\hat{\boldsymbol{u}}\hat{\boldsymbol{u}}} \rangle \tag{2}$$

is of particular importance. The symbol $\overline{\ldots}$ refers to the symmetric traceless part of a tensor, e.g., one has $\overline{\boldsymbol{ab}} = \frac{1}{2}(\boldsymbol{ab} + \boldsymbol{ba}) - \frac{1}{3}\boldsymbol{a} \cdot \boldsymbol{b}\boldsymbol{\delta}$ for the dyadic constructed from two vectors $\boldsymbol{a}$ and $\boldsymbol{b}$; $\boldsymbol{\delta}$ is the unit tensor. A viscous flow gives rise to a flow alignment [5–7] which can be detected optically via its ensuing birefringence. The alignment, in turn, affects the viscous flow [7,8] and consequently the friction pressure tensor $\boldsymbol{p}$ contains a contribution $\boldsymbol{p}_\mathrm{a}$ associated with the alignment, more specifically,

$$\boldsymbol{p} = -2\eta_\mathrm{iso}\boldsymbol{\gamma} + \boldsymbol{p}_\mathrm{a} \, , \tag{3}$$

$$\boldsymbol{p}_\mathrm{a} = -3nk_\mathrm{B}TRl_0^{-1} \int_0^L \boldsymbol{a}(t, s) \, \mathrm{d}s \, , \tag{4}$$

where η_iso is the "isotropic" viscosity for $\boldsymbol{a} = 0$ and $\boldsymbol{\gamma}$ is the symmetric traceless part of the velocity gradient tensor (shear rate tensor). In (4), n and T are the bead number density and the temperature of the liquid and l_0 is the effective length[#1] of a segment of the polymer chain, i.e., $l_0^{-1} \int_0^L \mathrm{d}s = N$ where N is the number of beads in one chain. The relation between $\boldsymbol{p}_\mathrm{a}$ and $\boldsymbol{a}$ which has been derived by Giesekus [8] and used by Doi and Edwards [3] is a limiting expression for long and thin segments which corresponds to $R = 1$ in eq. (4). In general the factor R occurring in (4) is the ratio of two transport coefficients [7,10]. For a comparison with expressions given in refs. [7,10] it should be noticed that the alignment tensor used there differs from (2) by a factor

[#1] For a quantitative analysis, the effective length l_0 stands for a persistence length or the length of a Kuhn element, viz. the bead distance, and cannot be replaced by the distance between neighboring monomers within one chain. See [9].

$(15/2)^{1/2}$. Curtiss and Bird [4] replaced the factor $3R$ by 1 and presented additional contributions to $\boldsymbol{p}_a$ associated with the "link tension" which are similar to those derived from constraint forces within the chain [11]. These terms are disregarded here.

An equation of change for $\boldsymbol{a}$ and consequently $\boldsymbol{p}_a$ can be derived from the kinetic equation for the distribution function f to be considered next.

2.2. Kinetic equation

The kinetic equation for $f = f(t, s, \hat{\boldsymbol{u}})$ is written as

$$\frac{\partial f}{\partial t} = -\boldsymbol{\omega} \cdot \mathscr{L} f - \mathscr{L} \cdot (\boldsymbol{T} f) + \mathscr{D}(f) , \tag{5}$$

with

$$\mathscr{L} := \hat{\boldsymbol{u}} \times \frac{\partial}{\partial \hat{\boldsymbol{u}}} = \boldsymbol{u} \times (\boldsymbol{\delta} - \hat{\boldsymbol{u}}\hat{\boldsymbol{u}}) \cdot \frac{\partial}{\partial \boldsymbol{u}} . \tag{6}$$

In (5), $\boldsymbol{\omega} := \frac{1}{2} \nabla \times \boldsymbol{v}$ is the vorticity associated with the flow field $\boldsymbol{v}$, and $\boldsymbol{T}$, which stems from the orienting torque exerted by the flow, is given by

$$\boldsymbol{T} := \tfrac{1}{2} R \mathscr{L} (\overline{\hat{\boldsymbol{u}}\hat{\boldsymbol{u}}} : \boldsymbol{\gamma}) , \qquad \boldsymbol{\gamma} := \overline{\nabla \boldsymbol{v}} . \tag{7}$$

The coefficient R depends on the "shape" of a particle [5,7,10]; $\boldsymbol{u} = l_0 \hat{\boldsymbol{u}}$ is the vector between neighboring beads. The term $\mathscr{D}(f)$ describes the "damping", which guarantees that f approaches the isotropic distribution $f_0 = (4\pi)^{-1}$ in the absence of orienting torques. The kinetic equation of Peterlin and Stuart [5] for solutions of rod-like particles (where the variable s is not needed) is of the form (5) with (6), (7) and

$$\mathscr{D}(f) = \mathscr{D}_{or}(f) \equiv w \mathscr{L}^2 f , \tag{8}$$

where w stands for the orientational diffusion coefficient. With an additional torque caused by a mean field taken into account in (7), such a kinetic equation has also been applied to the flow alignment of liquid crystals [10]. The reptation model damping term of Doi and Edwards [3] can be written as

$$\mathscr{D}(f) = \mathscr{D}_{rep} \equiv D \frac{\partial^2}{\partial s^2} f , \tag{9}$$

with a translational diffusion coefficient D. This term describes the change of the orientation of the segments caused by a one-dimensional diffusion of a polymer chain through its "tube".

We now consider the general case where both mechanisms of diffusion are taken into account, i.e. we set

$$\mathscr{D}(f) = \mathscr{D}_{\text{rep}} + \mathscr{D}_{\text{or}} . \tag{10}$$

The equivalence of the diffusion equation of Bird et al. [12] (19.3-26) and the Fokker-Planck equation (5) in the case of long and thin segments ($R = 1$) follows with the identity:

$$\begin{aligned} &\frac{\partial}{\partial \hat{\boldsymbol{u}}} \cdot [(\nabla \boldsymbol{v})^{\dagger} \cdot \hat{\boldsymbol{u}} - (\nabla \boldsymbol{v})^{\dagger} : \hat{\boldsymbol{u}}\hat{\boldsymbol{u}}\hat{\boldsymbol{u}}] f \\ &\quad = -(\nabla \boldsymbol{v})^{\dagger} : \hat{\boldsymbol{u}} \frac{\partial}{\partial \hat{\boldsymbol{u}}} f + [(\nabla \boldsymbol{v})^{\dagger} : \hat{\boldsymbol{u}}\hat{\boldsymbol{u}}]\left(3 + \hat{\boldsymbol{u}} \cdot \frac{\partial}{\partial \hat{\boldsymbol{u}}}\right) f \\ &\quad = -\boldsymbol{\omega} \cdot \mathscr{L} f - \mathscr{L} \cdot (\boldsymbol{T} f) . \end{aligned} \tag{11}$$

Instead of the two independent diffusion coefficients D and w, Bird introduces a reptation coefficient ϵ' and a time constant λ_{Bird}, which are related to the diffusion constants mentioned above (for comparison with the present notation):

$$\epsilon' = \frac{w}{D l_0^{-2} + w} , \qquad \lambda_{\text{Bird}} = \frac{L^2}{D + w l_0^2} . \tag{12}$$

The theory of Doi and Edwards [3] hence follows in a special case, the "reptation limit", where the orientational diffusion is more hindered than the one-dimensional diffusion, i.e.

$$\epsilon' = w = 0 \qquad \text{and} \qquad \lambda_{\text{Bird}} \to \lambda_{\text{Doi}} = \frac{L^2}{D} , \tag{13}$$

where λ_{Doi} is the time constant of the Doi and Edwards model.

An equation of change for the alignment tensor which is associated with the pressure tensor, cf. (4), is stated next as it can be obtained from the kinetic equation (5).

2.3. *Equation of change for the alignment tensor*

Multiplication of (5) with $\overline{\hat{\boldsymbol{u}}\hat{\boldsymbol{u}}}$ and integration over $\hat{\boldsymbol{u}}$ yields an equation for the second rank tensor $\boldsymbol{a}$,

$$\left(\frac{\partial}{\partial t} + \tau^{-1} - D \frac{\partial^2}{\partial s^2}\right) \boldsymbol{a} = \tfrac{2}{5} R \boldsymbol{\gamma} + \cdots , \tag{14}$$

with $\tau = (6w)^{-1}$. The dots stand for terms involving products of $\boldsymbol{a}$ with the vorticity $\boldsymbol{\omega}$ and the shear rate tensor $\boldsymbol{\gamma}$, as well as a term which couples $\boldsymbol{a}$ with an alignment tensor of rank 4. These terms can be inferred from [10]; they are of importance for the non-Newtonian viscosity and the normal pressure differences [7,8,12]. For an analysis of the frequency dependence of the viscosity in the Newtonian regime, these terms can be disregarded.

The complex viscosity $\eta_a \equiv \eta(\omega) = \eta' - i\eta''$ of a viscoelastic medium can be determined by measurements under an oscillatory shear flow (or deformation),

$$\boldsymbol{\gamma} \sim e^{-i\omega t} . \tag{15}$$

The relaxation of the material causes a phase shift δ between the (complex) stress $\boldsymbol{p}$ and the deformation $\boldsymbol{\gamma}$, which is related to the complex viscosity ($\tan\delta := \eta'/\eta''$), or alternatively, to the storage (G') and loss modulus (G'') via $G = G' + iG'' := i\omega\eta$. With the ansatz

$$\boldsymbol{a} = \tfrac{2}{5} R \boldsymbol{\gamma} C , \tag{16}$$

the scalar function $C = C(\omega, s)$, which has the dimension of time, obeys the equation

$$(\tau^{-1} - i\omega)C - D\,\frac{\partial^2 C}{\partial s^2} = 1 , \tag{17}$$

according to (14). The desired viscosity can be inferred from (4) and (16) with the solution C of (17).

2.4. *Frequency dependence of the viscosity*

The boundary condition proposed by Doi and Edwards [3] and also used by Curtiss and Bird [4] and Öttinger [13] are random orientations for the chain ends, i.e.,

$$f(s = 0, \hat{\boldsymbol{u}}) = f(s = L, \hat{\boldsymbol{u}}) = 1/4\pi \qquad \text{for all times} . \tag{18}$$

This implies $\boldsymbol{a} = 0$ and consequently $C(\omega, s = 0) = C(\omega, s = L) = 0$ (for all frequencies ω).

We introduce a model which takes into account the property of chain ends to participate in the flow alignment of the complete chain. Working out this modification, we set

$$C(\omega, s = 0) = C(\omega, s = L) = \tau_{\text{end}} , \tag{19}$$

in order to introduce a corresponding parameter τ_{end} with dimension of time, which is limited ($|\tau_{end}| < 5/(2R|\boldsymbol{\gamma}|)$) according to the possible values of the alignment tensor $\boldsymbol{a}$, and frequency-dependent in full generality. The physical evidence for such an anisotropic behavior under viscous flow will be shown in section 2.5 by use of NEMD computer-simulation results. The restriction (18) was helpful to solve (5) in a closed form [3,4], but with a side glance on (14) we can cancel the strong condition (18) at the end segments to derive the alignment tensor and hence the flow properties.

It is worth pointing out that the solution of (17), evaluated subject to the boundary condition (18) or (19) with $\tau_{end} = 0$, reproduces the viscosity of Doi and Edwards.

The solution of (17) subject to (19) is

$$C(\omega, \sigma) = \lambda\{1/z^2 + (1/z^2 - g)[\tanh(\tfrac{1}{2}z)\sinh(\sigma z) - \cosh(\sigma z)]\}\,, \tag{20}$$

where the variable $\sigma = L^{-1}s$ with $0 \leqslant \sigma \leqslant 1$ and $\lambda := \lambda_{Doi}$ is used; z is given by

$$z := \sqrt{\tau^{-1}\lambda - i\omega\lambda} \tag{21}$$

and

$$g := \tau_{end}\lambda^{-1} \tag{22}$$

is the dimensionless parameter for the chain ends, which determines the characteristic features of C.

From (4) and (16) one infers

$$\boldsymbol{p}_a = -2\eta_a\boldsymbol{\gamma}\,, \tag{23}$$

where the viscosity $\eta_a(\omega)$ associated with the alignment is given by

$$\eta_a(\omega) = G_a \int_0^1 C\,d\sigma\,, \tag{24}$$

with the "alignment" shear modulus

$$G_a = \tfrac{3}{5}R^2 N n k_B T\,, \tag{25}$$

which, for $R = 1$, reduces to the expression given by Doi [3]. Now insertion of (20) into (24) yields, with the simplified notation $\eta \equiv \eta_a$,

$$\eta(\omega) = G_a\lambda\left[\frac{1}{z^2} + \left(g - \frac{1}{z^2}\right)\frac{2\tanh(\frac{1}{2}z)}{z}\right]. \tag{26}$$

Limiting expressions for $z \to 0$ and $z \to \infty$ are $\eta \to G_a\lambda(\frac{1}{12} + g)$ and $\eta \to G_a\lambda(2gz^{-1} + z^{-2})$, respectively. For a situation (e.g., a dilute solution) where the orientational relaxation rate τ^{-1} is much larger than the diffusional relaxation rate λ^{-1}, the latter asymptotic expression leads to the Maxwell model type expression $\eta(\omega) = G_a(1 - i\omega\tau)^{-1}$, which does not involve $\lambda \sim D^{-1}$.

For polymeric melts and highly concentrated solutions where the reorientational motion is strongly hindered, one expects the opposite situation, viz. $\tau^{-1} \ll \lambda^{-1}$. The pure reptation model considered in [3,4] corresponds to $\tau^{-1}\lambda \to 0$ and consequently $z \to y$ with

$$y := (-i\omega\lambda)^{1/2} = (1 - i)\Omega^{1/2}, \qquad \Omega := \tfrac{1}{2}\omega\lambda. \tag{27}$$

In this case (26) reduces to

$$\eta(\omega) = \eta_{DE}[H_{DE}(\omega) + H_{end}(\omega)], \tag{28}$$

with the Doi–Edwards viscosity

$$\eta_{DE} = \tfrac{1}{12}G_a\lambda = \tfrac{1}{20}Nnk_BT\lambda \tag{29}$$

and the dimensionless damping functions

$$H_{DE} = 12\frac{1}{y^2}\left[1 - \frac{2}{y}\tanh(\tfrac{1}{2}y)\right], \tag{30}$$

$$H_{end} = g\frac{24}{y}\tanh(\tfrac{1}{2}y). \tag{31}$$

The index 'end' labels a term, which vanishes for $g = 0$, and represents the influence of flow-aligned chain ends on the frequency behavior of the viscosity. Decomposition of the coefficient H_{DE} into real and imaginary parts according to $H = H' + iH''$ yields

$$\begin{aligned} H'_{DE} &= 6\Omega^{-3/2}(\sinh\Omega^{1/2} - \sin\Omega^{1/2})B, \\ H''_{DE} &= 6\Omega^{-1}[1 - \Omega^{1/2}(\sinh\Omega^{1/2} + \sin\Omega^{1/2})]B, \\ B &:= (\cosh\Omega^{1/2} + \cos\Omega^{1/2})^{-1}. \end{aligned} \tag{32}$$

Although it is not obvious at first glance, the result (32) is equivalent to the

series expression

$$H = \sum_{\text{odd}\alpha} H_\alpha \frac{1}{1 - i\omega\lambda_\alpha} , \tag{33}$$

with $H_\alpha = 96\pi^{-4}\alpha^{-4}$, $\lambda_\alpha = \pi^{-2}\alpha^{-2}\lambda$, which has been derived by Curtiss and Bird [4].

Despite the fact that (29) is very appealing since the reptation model leads in a rather plausible way [3,4] to a dependence of the viscosity on the degree of polymerization N (or equivalently on the molecular weight) which is close to the experimentally observed behavior, the frequency dependence as given by (32) or (33) is not satisfactory. The decrease of the real part of the viscosity with increasing frequency, e.g., is in most cases by far not as strong [12] as the $\Omega^{-3/2}$ decrease predicted by (32). This deficiency is overcome by the additional term H_{end} in (28), which involves the factor g, cf. (31), which characterizes the alignment of the chain ends.

Nonequilibrium molecular dynamics (NEMD) computer-simulation results, which show that this end alignment is indeed nonzero, are discussed next.

2.5. *NEMD simulation*

The NEMD computer simulations have been performed (with a Cray-XMP) for chains with 32 beads in systems with a total number of 128 (resp. 512) beads in a simulation cell with periodic boundary conditions, in order to avoid boundary layer effects. The equations of motion of N_{tot} beads with mass m have been integrated numerically by a (5th order) Gear–predictor–corrector algorithm. The Lennard-Jones potential

$$\phi = \phi_{\text{LJ}} = 4\epsilon\left[\left(\frac{\sigma}{r}\right)^{12} - \left(\frac{\sigma}{r}\right)^{6}\right] \quad \text{for } r \leqslant 2.5\sigma \quad \text{and} \quad \phi = 0 \quad \text{for } r > 2.5\sigma , \tag{34}$$

is increased by a factor 100 for the interaction between those beads, which are nearest neighbors in one chain. The characteristic energy ϵ and the typical molecular length σ, together with the mass m of a bead, are, as usual, used to express all physical quantities in reduced units. The volume V of the basic periodicity box is determined by N_{tot} and the bead number density $n = N_{\text{tot}}/V$. The temperature T is kept constant by rescaling the magnitude of the peculiar velocities. Additional constraints are imposed in order to simulate a plane Couette flow,

$$\boldsymbol{\gamma} = \gamma \overline{\boldsymbol{e}_x \boldsymbol{e}_y} ,$$

with the velocity $\boldsymbol{v}$ in the x-direction and its gradient in the y-direction;

$$\gamma = \frac{\partial v_x}{\partial y} \tag{35}$$

is the shear rate. The quantity of interest here is the alignment tensor

$$\boldsymbol{a}(s, t) := \langle \overline{\hat{\boldsymbol{u}}\hat{\boldsymbol{u}}} \rangle , \tag{36}$$

specifying the orientation of a segment at position s within a chain. For a plane Couette geometry, only 3 of the 5 independent components are nonzero, viz.

$$a_+ = \langle \hat{u}_x \hat{u}_y \rangle , \qquad a_- = \tfrac{1}{2} \langle \hat{u}_x \hat{u}_x - \hat{u}_y \hat{u}_y \rangle , \qquad a_0 = \langle \hat{u}_z^2 - \tfrac{1}{3} \rangle , \tag{37}$$

which depend only on s and γ in the stationary regime and have been extracted from the NEMD simulation. In order to show the nonvanishing anisotropy of the whole chain under shear flow, we plotted the components of $\boldsymbol{a}$ against the relative position $\sigma = s/L$ within the chain for a set of shear rates in fig. 1. The finite values of the components a_k $(k = +, -, 0)$ for $\sigma = 0$ and $\sigma = 1$ imply the flow-induced alignment of the chain ends.

A quantitative comparison of the NEMD-simulation result for the real quantity $a_+(\gamma, \sigma)$ with our calculation of the complex component $a_+(\omega, \sigma)$ of the alignment tensor, cf. (20) with (16), is possible by generalizing the Cox–Merz rule [14]:

$$\eta(\gamma) \sim |\eta(\omega \to \gamma)| , \tag{38}$$

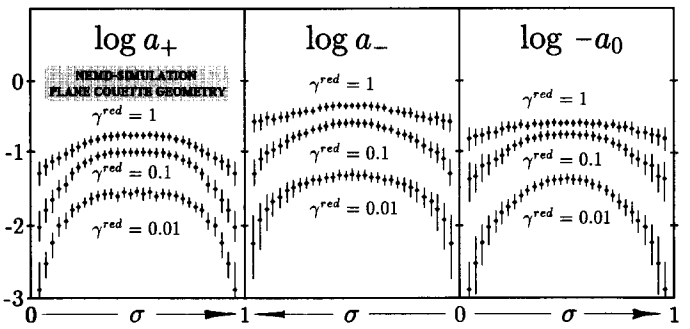

Fig. 1. NEMD computer-simulation data of the alignment tensor components a_k $(k = +, -, 0)$ (eq. (37)) as functions of σ for a stationary plane Couette geometry with various shear rates γ. The variable σ denotes the relative position of a segment vector $\boldsymbol{u}$ within the chain. The finite values of the a_k at $\sigma = 0$ and $\sigma = 1$ imply a flow induced alignment of the chain ends.

which has been experimentally verified [15]. The suitable generalization for the alignment tensor is

$$a_+(\gamma, \sigma) \sim \gamma |a_+(\omega \to \gamma, \sigma)| , \tag{39}$$

since – together with our result (16), (20) for the alignment tensor – the stated proportionality (39) leads to the numerical validity of the Cox–Merz rule (38) if the quantity g is small, i.e., $g \ll 1$. This follows from the approximative relation (take C from eq. (20))

$$\left| \int C \, \mathrm{d}\sigma \right| \approx \int |C| \, \mathrm{d}\sigma . \tag{40}$$

The dependence of the alignment tensor component $a_+(\gamma, \sigma)$ on both the shear rate and the relative position within one chain for three values of g have been plotted in fig. 2. For $g \neq 0$, the behavior is similar to the observation made by NEMD-computer simulations (see fig. 1).

The pronounced alignment of chain ends under shear flow we have already detected in a "small" system, e.g. in a periodicity cell with 4 chains, built up by 32 beads, where the crossover from Rouse- to reptation dynamics, as studied numerically by Kremer and Grest [16], has not been reached. However it is conjectured that the alignment of the end segments is also of crucial importance for longer chains. The NEMD computer simulations show a smooth dependence of the alignment on the segment position σ (see fig. 1) and thus do not support the assumption of an approximate freedom of the orientations of the end segments, made in refs. [3,4,12,13].

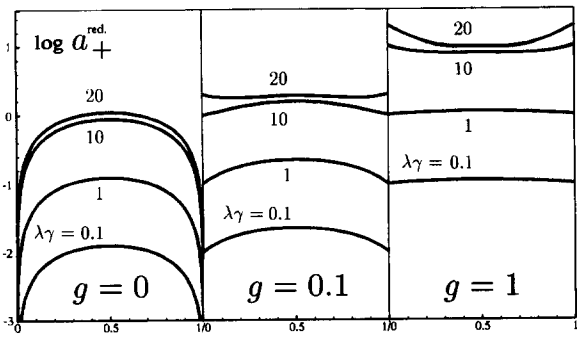

Fig. 2. The dependency of the alignment tensor component a_+^{red} as defined on the lhs of (39) on the relative position within one chain σ, the parameter g and the dimensionless shear rate has been computed theoretically from eqs. (16), (20), (39). The NEMD-computer simulation result (see fig. 1) is consistent with the calculation only for a nonvanishing parameter g which is associated with the flow-induced alignment of the chain ends.

Notice that for shear rates greater than an "inversion" shear rate, the alignment tensor component a_+ for an end-segment of a chain ($\sigma = 0$ or $\sigma = 1$) is greater than a_+ in the centre of a chain. The dependence of this shear rate γ_{inv} on the parameter g can be calculated from (20) by solving the equation $C(0, \gamma_{inv}) = C(\frac{1}{2}, \gamma_{inv})$ for γ_{inv}. Its existence is not in contradiction with a preferred alignment of the middle parts of a chain in the direction of the flow velocity, i.e., a maximum of the component a_- at $\sigma = 0.5$. To detect the "inversion" shear rate, whose existence is in sharp contradiction to the assumptions made by several authors (see section 2.4 or compare with the plot "$g = 0$" in fig. 2), we consider enlarging our NEMD simulation to longer chains. Then it will be possible to determine g and its dependence on the chain length from NEMD-simulation data at low shear rates by comparing the strength of alignment at the chain ends with the strength of alignment in the middle parts of the chains.

In section 2.6 we will discuss the dependence of g and the time constant λ on the chain length as obtained from an experimental result.

Results for the components a_- and a_0 from NEMD simulations in fig. 1 show that the shear rate dependence of the corresponding normal pressure differences (resp. the viscometric functions, (see (4)), based on a Fokker–Planck approach, should be calculated more carefully as was done before, since the condition (18) for the chain ends leads to vanishing components a_-, a_0 for $s = \sigma = 0$.

2.6. *The effect of flow-induced alignment of chain ends*

As a next step. we will discuss the features of the storage (G') and loss (G'') modulus as given by

$$G = G' + \mathrm{i}G'' := \mathrm{i}\omega\eta\,, \tag{41}$$

with η from (28). The complex shear modulus G (41) includes the quantity τ_{end} for the chain ends, introduced by (19). After a remark about the limiting expressions for low and high frequencies, we will show how to determine the parameter τ_{end}, the time constant λ and the shear modulus G_a from experimental data in section 3. For a quick overview, we will calculate the interrelation between τ_{end} or alternatively g and the width of the plateau region.

From a Taylor series of the hyperbolic function in (30), (31) follows

$$\lim_{\omega\to 0} G' = G_a \tfrac{1}{12}(\tfrac{1}{10} + g)(\omega\lambda)^2\,, \tag{42}$$

$$\lim_{\omega\to 0} G'' = G_a(\tfrac{1}{12} + g)(\omega\lambda)^1\,. \tag{43}$$

For high frequencies ω, the analytic expressions are

$$\lim_{\omega\to\infty} G' = G_a[(1-\delta_{g,0})\sqrt{2}\, g(\omega\lambda)^{1/2} + \delta_{g,0}]\,, \tag{44}$$

$$\lim_{\omega\to\infty} G'' = G_a[(1-\delta_{g,0})\sqrt{2}\, g(\omega\lambda)^{1/2} + \delta_{g,0}\sqrt{2}\,(\omega\lambda)^{-1/2}]\,. \tag{45}$$

Here, δ stands for the usual Kronecker symbol. A nonvanishing anisotropic parameter g leads to a qualitative change in the frequency behavior of polymeric melts.

In distinction to the Doi–Edwards theory ($g = 0$), for high frequencies the presented modification predicts one region, where both moduli display the same characteristics, independent of $g = g(\omega)$, and another (plateau) region, where the storage modulus is nearly constant within a frequency range, which depends only on g. In a wide region of frequencies, the assumption of a constant value of g leads to a good approximation, as we have substantiated from NEMD-simulation results. The experimental data of various authors are described very well even for the simple case, where g is constant (but material dependent), cf. section 3. From a microscopic point of view, the possibility of (physical) chain ends to align under shear flow is connected with the time $\tau_{\text{end}} = g\lambda$, as stated in (19). For λ see (12) and (13). Its dependence on the molecular weight is discussed in [12]. Therefore we expect a characteristic viscous scenario for a variation of the molecular weight (resp. the chain length N), because g strongly affects the physical behavior of the viscosity. The molecular weight dependence, found e.g. by Onogi et al. [17], can be interpreted by setting $\lambda \sim N^{3.4}$. A fit of the experimental data is consistent with

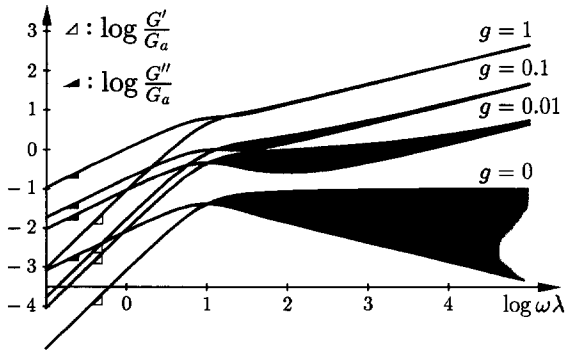

Fig. 3. The shear moduli G' and G'' as functions of the frequency ω for various values of the parameter g, cf. eq. (41) and (28).

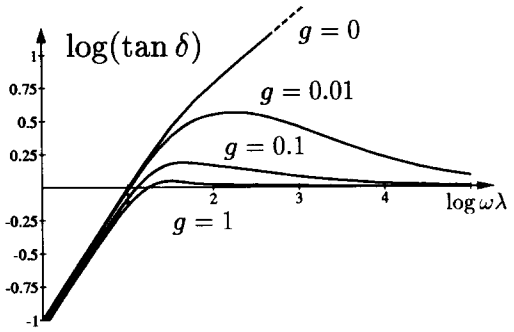

Fig. 4. The phase shift δ between (complex) stress and deformation as functions of the frequency ω for various values of the parameter g.

$g \sim N^{-2.4}$, which implies $\tau_{\text{end}} \sim N^1$ ([18][#2] and eq. (50)). For the meaning of the plateau in G' and a discussion of the results, obtained by Onogi et al., see Larson [19].

For a plot of G' (G'') see fig. 3; the phase shift δ for different values of g is shown in fig. 4. Notice that the curves G' and G'' tend to overlap with increasing values for the shear frequency. The positive slope of G' and G'' at high frequencies ω follows here without the recourse to "glassy relaxation modes", as suggested by Ferry [20].

3. Comparison between theory and experiments

In this section it is shown how the theory describes the experimental results and how one can extract the physical quantities of interest.

Following the textbook of Larson [19], we compare experimental data, obtained for polymeric melts and concentrated solutions, with theoretical results, obtained by de Gennes [21], Doi [22] and with our result. In order to test the validity of our predictions over a wide range of frequencies which includes the full plateau region, we have chosen first a set of experimental data, presented by Ferry (data from Masuda et al. [24]). Together with the measured values in fig. 5, we give both the theoretical curves according to (41) and (28), which take into consideration the proposed anisotropy of chain ends, and the results obtained by Doi and Edwards [3], Curtiss and Bird [4,12], de Gennes [21] and Doi [22]. There are three basic theoretical quantities: g, λ and G_a, needed to calculate the theoretical curves shown in fig. 5; for their specific

[#2] See section 3, fig. 7 for the width of the plateau region, and Larson [19] section 4.3.2 for discussion of the data.

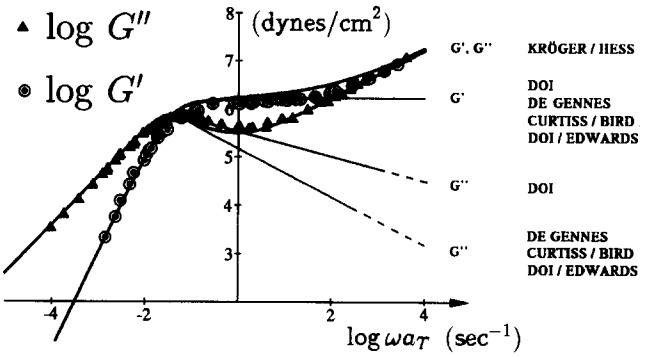

Fig. 5. Comparison of theory and experiment for the loss and storage moduli. The experimental measurements by Masuda, Kitagawa, Inoue and Onogi [24] have been performed on a monodisperse polysterene melt ($M_w = 215000$). The moduli are functions of shear rate reduced to a reference temperature of $T^{red} = 160°C$ by a factor a_T. The (upper) traced lines pertain to the theoretical parameters $G_a = 1.7 \times 10^6$ dyn cm^{-2}, $\lambda = 260$ s and $\tau_{end} = g\lambda = 1$ s in (31). The theoretical curves for $g = 0$ corresponding to the results of Doi and Edwards [3], Curtiss and Bird [4], and de Gennes [21] are also shown. The calculation of Doi [22] takes into account fluctuations in the length of the "primitive chain".

values see the figure caption. In the figure we do not compare our result with theoretical approaches, which involve a large set of parameters, e.g. relaxation frequency analysis.

The set of quantities, which characterize the experimental data, are schematically drawn in fig. 6. Only two of the four frequencies ω', ω'', ω_s and ω_r are independent.

Due to the geometry of fig. 6 the identity

$$\omega_s^2 = (\omega')^2 \frac{\omega'}{\omega''} \tag{46}$$

holds true. To test the set of measured characteristic frequencies, (46) is helpful. The few steps to calculate all the theoretical quantities within the given approach can be inferred from (41), (28) and fig. 6:

$$g = g(\omega_s, \omega'') = \frac{1}{11}\left(\frac{1}{1-(6\omega''/\omega_s)^{1/2}} - 1\right), \tag{47}$$

$$\omega_s \lambda = 10 \frac{(1+12g)}{(1+10g)}, \tag{48}$$

$$G_a G_s^{-1} = \frac{12}{10} \frac{(1+10g)}{(1+12g)^2}, \tag{49}$$

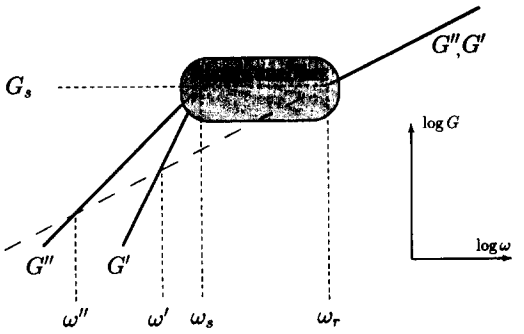

Fig. 6. Schematic plot of the real and imaginary part of the complex shear modulus explains the important quantities which characterize the frequency dependence. At higher frequencies, $G' \sim \omega^0$, $G'' \sim \omega^{-1}$ is expected but not displayed in fig. 6.

with the experimental plateau modulus G_s. For a quick overview and in order to get a feeling for the connection between the new quantity g and the width of the plateau region $(\omega_r - \omega_s)$, respectively the relation between the two frequencies ω'' and ω_s, we have plotted both curves in fig. 7. For the dimensionless ratio ω_r/ω_s, which also measures the width of the plateau region and can be extracted from a given experimental result with better accuracy than the difference $\omega_r - \omega_s$, we get

$$\log \frac{\omega_r}{\omega_s} = \frac{5}{144}\, g^{-2}\, \frac{(1+12g)^3}{(1+10g)} \,. \tag{50}$$

The present theory can also be applied to concentrated polymer solutions. In fig. 8 experimental data of Holmes et al. ([25] or see Larson [19]) for three different concentrations are compared with our result. Again an excellent

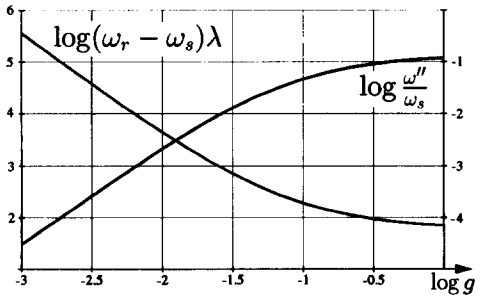

Fig. 7. The (dimensionless) length of the plateau region $(\omega_r - \omega_s)\lambda$ and the ratio ω''/ω_s of the characteristic frequencies defined through fig. 6 as functions of the parameter g.

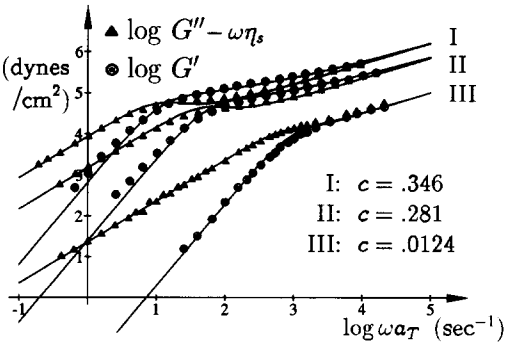

Fig. 8. Comparison of theory and experiment for the loss and storage moduli versus frequency for polysterene of molecular weight 267 000 dissolved in chlorinated diphenyl at the concentrations c shown (in gm/cm^3) (from Holmes, Kusamizu, Osaki and Ferry [25]). The three traced lines pertain to the theoretical parameters: $G_a = (80\,000 | 55\,000 | 450)$ dyn/cm^2, $\lambda = (0.8 | 0.178 | 0.01)$ s, $\tau_{end} = (0.04 | 0.012 | 0.05)$ s for $c = (0.346 | 0.281 | 0.0124)$.

agreement between experiment and theory can be obtained. For the values of the chosen g, λ, G_a see the figure caption.

4. Concluding remarks

In this paper, it has been demonstrated that a Fokker–Planck approach with appropriate boundary conditions for the chain ends can be applied to study the rheological properties of fluids composed of long chain molecules. Computer simulations [23] can yield some new insight into the dynamic processes in polymeric liquids and substantiate a modification of a well known theory. We have introduced a material dependent quantity τ_{end} with dimension of time for the alignment of chain ends, including the physical or chemical peculiarities of a given polymeric fluid. The presented method can be applied to predict a change in the viscoelastic behavior for polymeric melts and concentrated solutions during a variation of the flexibility of chain ends and the time "constant" λ, which is connected with the molecular weight. Even for very high frequencies, when the parameter for the alignment of chain ends τ_{end} (with dimension of time) should tend to be frequency dependent, the excellent agreement with experimental results, found on the basis of the Fokker–Planck description, provides undoubted evidence about the validity of this method.

Our result for the complex viscosity – combined with the Cox–Merz rule [14] – yields a shear rate dependence of the non-Newtonian viscosity, which qualitatively agrees well with the experimentally observed shear thinning. The empirical Cox–Merz rule is not needed if one extends the present approach to

the nonlinear flow regime. This seems to be feasible and will then allow a similar comparison between theory and measurements of the viscosity and the normal pressure differences.

Acknowledgements

This work has been performed under the auspices of the Sonderforschungsbereich 335 "Anisotropic Fluids". Financial support is gratefully acknowledged.

References

[1] S.F. Edwards, Proc. Phys. Soc. London 92 (1967) 9.
[2] P.G. de Gennes, J. Chem. Phys. 55 (1971) 572.
[3] M. Doi and S.F. Edwards, J. Chem. Soc. Faraday Trans. II 74 (1978) 1789, 1802, 1818; 75 (1979) 38.
[4] C.F. Curtiss and R.B. Bird, J. Chem. Phys. 74 (1981) 2016, 2026.
[5] A. Peterlin and H.A. Stuart, Hand- und Jahrbuch d. Chem. Phys., A. Eucken and K.I. Wolf, eds., 8 (1943) 113.
[6] J.W.M. Noordermeer, R. Daryanani and H.R.K.N. Janeschitz-Kriegel, Polymer 17 (1976) 155.
[7] S. Hess, Physica A 86 (1977) 383; 87 (1977) 273; 112 (1982) 287.
[8] H. Giesekus, Rheol. Acta 2 (1962) 50.
[9] P.J. Flory, Principles of Polymer Chemistry (Cornell Univ. Press, Ithaca, NY, 1953).
W. Kuhn, Kolloid Z. 76 (1936) 258; 87 (1939) 3.
[10] S. Hess, Z. Naturforsch. A 31 (1976) 1034.
[11] M. Kröger, Diplomarbeit, TU Berlin (1991), unpublished.
[12] R.B. Bird, R.C. Armstrong and O. Hassager, Dynamics of Polymeric Liquids, vol. 1, Fluid Mechanics (Wiley, New York, 1987).
Dynamics of Polymeric Liquids, vol. 2, Kinetic Theory (Wiley, New York, 1987).
[13] H.C. Öttinger, J. Chem. Phys. 91 (1989) 6455.
[14] W.P. Cox and E.H. Merz, J. Polym. Sci. 28 (1958) 619.
[15] W.M. Kulicke, Fließverhalten von Stoffen und Stoffgemischen (Hüthing & Wepf, Basel, Heidelberg, New York, 1986) p. 24.
[16] K. Kremer and G.S. Grest, J. Chem. Phys. 92 (1990) 5057.
[17] S. Onogi, T. Masuda and K. Kitagawa, Macromolecules 3 (1979) 109.
[18] M. Kröger and S. Hess, in: Theoretical and Applied Rheology (Elsevier, Amsterdam, 1992) p. 422.
[19] R.G. Larson, Constitutive Equations for Polymer Melts and Solutions (Butterworths, London, 1988) 99 pp.
[20] J.D. Ferry, Viscoelastic Properties of Polymers, 3rd ed. (Wiley, New York, 1980).
[21] P.G. de Gennes, Scaling Concepts in Polymer Physics (Cornell Univ. Press, Ithaca, NY, 1979) ch. 2.
[22] M. Doi, J. Polym. Sci. Poly. Phys. Ed. 21 (1983) 667.
[23] S. Hess, J. Non-Newtonian Fluid Mech. 23 (1987) 305.
[24] T. Masuda, K. Kitagawa, I. Inoue and S. Onogi, Macromolecules 3 (1970) 109.
[25] L.A. Holmes, S. Kusamizu, K. Osaki and J.D. Ferry, J. Polym. Sci. A2, 9 (1971) 2009.